# Influence of initial-state momentum anisotropy on the final-state collectivity in small collision systems

Maowu Nie, <sup>1,2</sup> Li Yi, <sup>1</sup> Xiaofeng Luo, <sup>3</sup> Guoliang Ma, <sup>4,5,\*</sup> and Jiangyong Jia, <sup>6,3,†</sup>

<sup>1</sup> Institute of Frontier and Interdisciplinary Science, Shandong University, Qingdao 266237, China

<sup>2</sup> Key Laboratory of Particle Physics and Particle Irradiation, Ministry of Education, Shandong University, Qingdao, Shandong 266237, China

<sup>3</sup>Institute of Particle Physics, Central China Normal University, Wuhan 430079, China
<sup>4</sup>Key Laboratory of Nuclear Physics and Ion-Beam Application, Institute of Modern Physics, Fudan University, Shanghai 200433, China
<sup>5</sup>Shanghai Institute of Applied Physics, Chinese Academy of Sciences, Shanghai 201800, China
<sup>6</sup>Department of Chemistry, Stony Brook University, Stony Brook, New York 11794, USA



(Received 20 June 2019; published 16 December 2019)

A multiphase transport model is used to understand the origin of long-range collective azimuthal correlations in small-system collisions. To disentangle between collectivity associated with initial-state intrinsic momentum anisotropy and the collectivity arising as a final-state response to the collision geometry, we studied the development of collectivity in 5.02-TeV p+Pb collisions with both initial-state and final-state effects included. We find that the initial momentum anisotropy may not be fully isotropized through parton interactions, and the final-state partonic collectivity in general is correlated with both the initial momentum anisotropy and the shape of the collision geometry. The initial momentum anisotropy also influences the event-by-event fluctuation of collective flow. Therefore, the mere evidence of the geometry response of the collective flow cannot rule out the presence of large contributions from the initial state.

DOI: 10.1103/PhysRevC.100.064905

## I. INTRODUCTION

In high-energy hadronic collisions, particle correlation techniques are often used to probe the multi-parton dynamics of QCD in the strongly coupled regime [1]. Measurements revealed a strong azimuthal anisotropy in particle densities  $dN/d\phi \propto 1 + 2\sum_{n=1}^{\infty} v_n \cos n(\phi - \Psi_n)$ , where  $v_n$  and  $\Psi_n$  represent the magnitude and the phase of the nth-order harmonic, denoted by flow vector  $V_n = v_n e^{in\Psi_n}$  [2]. The azimuthal correlations are found to be collective, involving many particles over a wide pseudorapidity range. This azimuthal anisotropy was first observed in a large A+A collision system [2–5], but was then observed and studied in small collision systems such as pp and p+Pb collisions at the LHC [6–13] and p+Au, d+Au, and  $^3$ He+Au collisions at RHIC [14–18].

Although azimuthal anisotropy in A + A collisions is naturally explained as a result of hydrodynamic collective expansion of the hot and dense matter produced in the collision [19], the applicability of the hydrodynamic picture in small collision systems such as pp or p+A collisions remains an open question [20,21]. It has been argued that the size is too small and the lifetime is too short for the matter in a small system to hydrodynamize and approach local isotropization [22]. Instead, the azimuthal anisotropy may reflect intrinsic long-range momentum correlations of the dense gluon field

right after the collision [23–25]. The current debate is focused on the timescale for the emergence of collectivity: Is the collectivity born in the initial state, developed during nonequilibrium transport before the system hydrodynamizes, or does it arise even later when the system can be described by hydrodynamics? The latter two scenarios lead to a collectivity that correlates with the initial spatial eccentricities, while the first does not.

The system produced right after the collision is highly anisotropic in momentum space, and the strong interactions among the constituents of the produced system tend to isotropize this anisotropy [26,27]. However, the short lifetime may prevent the produced matter to fully isotropize before hadronization. In this case, the collectivity of final-state particles may have contributions from both initial momentum anisotropy and final-state geometry-driven anisotropy [21,28,29]. In this paper, we investigate the possibility and consequence of coexistence of initial-state and final-state effects using a transport model for p+Pb collisions at  $\sqrt{s_{\rm NN}}$  = 5.02 TeV. We show that the long-range azimuthal anisotropy for final-state particles could be strongly modified by the initial momentum anisotropy while it still maintains a strong correlation with the initial spatial eccentricity. We find that the short-range azimuthal anisotropy is sensitive to the microscopic mechanism for initial momentum anisotropy or finalstate nonequilibrium effects.

#### II. MODEL

The model used for this study is a multiphase transport (AMPT) model [30]. The AMPT model is successful in

<sup>\*</sup>glma@fudan.edu.cn

<sup>†</sup>jiangyong.jia@stonybrook.edu

describing several features of small-system collectivity at RHIC and the LHC, over a wide range of collision species and energies [31–34]. It starts with Monte Carlo Glauber initial conditions, and the space-time evolution of the collision is modeled via strings and jets that melt into partons, followed by parton scattering, parton coalescence, and hadronic scattering. The collectivity is generated mainly in the partonic scattering stage, known as the Zhang's parton cascade (ZPC), which leads to an azimuthal anisotropy of final particles correlated with the shape of the initial geometry. We use the setup of Ref. [34] with a partonic cross section of  $\sigma_p = 3$  mb.

In this paper, we focus on the leading component of azimuthal anisotropy, elliptic flow  $V_2 = v_2 e^{i2\Psi_2}$ . Since the number of particles in each event is finite, the  $V_2$  can only be estimated from the  $\phi$  angle of the particles,

$$\mathbf{q}_2 \equiv q_2 e^{i2\Psi_2^{\text{obs}}} = \langle e^{i2\phi} \rangle, \tag{1}$$

where the observed event plane (EP)  $\Psi_2^{obs}$  smears around the true EP angle  $\Psi_2$  due to statistical fluctuations.

In the final-state scenarios,  $V_2$  is driven by the eccentricity vector  $\mathcal{E}_2$ , which can be calculated from initial-state coordinates  $(r_i, \phi_i)$  of the participant nucleons

$$\mathcal{E}_2 \equiv \varepsilon_2 e^{i2\Psi_2^{\text{PP}}} = -\frac{\langle r^2 e^{i2\phi} \rangle}{\langle r^2 \rangle},\tag{2}$$

where the  $\Psi_2^{PP}$  is known as the participant plane (PP).

To precisely control the amount of initial momentum anisotropy, a two-step procedure is used to prepare partons entering the ZPC stage. We first randomize the  $\phi$  angle of all initial partons to eliminate any global initial momentum anisotropy (but the momentum distribution in local rest frame is generally anisotropic). This step also removes any azimuthal anisotropy associated with nonflow effects. We then rotate the parton  $\phi$  angle via the procedure described in Ref. [35] to produce a fixed amount of initial elliptic anisotropy along a random-event-wise direction  $V_2^{\rm ini} = v_2^{\rm ini} e^{i2\Psi_2^{\rm MP}}$  (where MP stands for momentum plane). This is obtained by modifying the azimuthal angle of each parton,  $\phi_0$ , to a new value  $\phi$  by solving the following equation:

$$\phi_0 \to \phi = \phi_0 - v_2^{\text{ini}} \sin 2(\phi - \Psi_2^{\text{MP}}).$$
 (3)

The  $\phi$  angle can be obtained via a simple numerical method. The partons with updated azimuthal angles then go through the ZPC and later stages of the AMPT model.

In this analysis, we focus on understanding the evolution of collectivity driven by the parton scattering processes. To this end, we calculate and compare the  $v_2$  before and after the ZPC using partons in  $0.3 < p_T < 3$  GeV for p+Pb collisions at  $\sqrt{s_{\rm NN}} = 5.02$  TeV. However, in order to relate to experimental measurements, we present the final results as a function of  $N_{\rm ch}$ , the number of charged particles in  $p_T > 0.4$  GeV and  $|\eta| < 2.5$ , after final hadronic transport.

The elliptic flow coefficient is calculated with both twoand four-particle correlation methods. In the two-particle correlation method, we calculate

$$c_2\{2\} = \langle \langle e^{i2(\phi_1^a - \phi_2^b)} \rangle \rangle = \langle v_2^2 \rangle, \tag{4}$$

where partons a and b are chosen from two subevents according to  $-2.5 < \eta_a < -\frac{2.5}{3}$  and  $\frac{2.5}{3} < \eta_b < 2.5$ , and the  $\langle\langle \ \rangle\rangle$  represent averaging over all pairs in one event, then over all events. The large gap between the two subevents reduces the short-range correlations. The flow coefficient from the two-particle cumulant,  $v_2\{2\} \equiv \sqrt{c_2\{2\}} = \sqrt{\langle v_2^2 \rangle}$ , measures the root-mean-square values of  $v_2$ . Similarly we also calculate  $v_2$  using four-particle correlations with the same two subevents [36]:

$$c_{2}\{4\} = \left\langle \left\langle e^{i2(\phi_{1}^{a} + \phi_{2}^{a} - \phi_{3}^{b} - \phi_{4}^{b})} \right\rangle - 2\left\langle \left\langle e^{i2(\phi_{1}^{a} - \phi_{2}^{b})} \right\rangle \right\rangle^{2}$$

$$= \left\langle v_{2}^{4} \right\rangle - 2\left\langle v_{2}^{2} \right\rangle^{2}. \tag{5}$$

From this we define the four-particle elliptic flow coefficient  $v_2$ {4} as

$$v_2{4} = (-c_2{4})^{1/4} = (2\langle v_2^2 \rangle^2 - \langle v_2^4 \rangle)^{1/4},$$
 (6)

which is sensitive to event-by-event fluctuation of elliptic flow. Following Refs. [37,38], we characterize the relative strength of flow fluctuation using a cumulant ratio,

$$nc_2{4} \equiv c_2{4}/c_2{2}^2 = -(v_2{4}/v_2{2})^4.$$
 (7)

To further quantify the influence of initial momentum anisotropy and geometry response to the final elliptic flow signal, we also perform a detailed study of the angular correlation between the MP or the PP and the EP of the final-state elliptic flow. The correlation between the PP and the EP is calculated as

$$\langle \cos 2(\Psi_2^{PP} - \Psi_2) \rangle = \sqrt{\frac{\langle \cos 2(\Psi_2^{PP} - \Psi_2^{obs,a}) \rangle \langle \cos 2(\Psi_2^{PP} - \Psi_2^{obs,b}) \rangle}{\langle \cos 2(\Psi_2^{obs,a} - \Psi_2^{obs,b}) \rangle}}, \quad (8)$$

where  $\Psi_2^{\text{obs},a}$  and  $\Psi_2^{\text{obs},b}$  are the observed EP in subevents a and b, respectively. The denominator represents a resolution factor, obtained from the correlation between the two subevents, which corrects for the smearing of observed EP from the true EP.

Similarly the correlation between the MP for the initial partons and the EP for the final partons is calculated as

$$\cos 2(\Psi_2^{MP} - \Psi_2) \rangle$$

$$= \sqrt{\frac{\langle \cos 2(\Psi_2^{MP} - \Psi_2^{\text{obs},a}) \rangle \langle \cos 2(\Psi_2^{MP} - \Psi_2^{\text{obs},b}) \rangle}{\langle \cos 2(\Psi_2^{\text{obs},a} - \Psi_2^{\text{obs},b}) \rangle}}. \quad (9)$$

# III. RESULT

The top and middle rows of Fig. 1 show the two-particle correlation function for partons in relative azimuthal angle  $\Delta\phi$  and pseudorapidity  $\Delta\eta$  before (top row) and after the ZPC (middle row). The correlation function is constructed in the highest multiplicity p+Pb collisions ( $N_{\rm ch}>150$ ) as the ratio between pair distribution from the same event and pair distribution from mixed events [10]. When the initial anisotropy is set to zero,  $v_2^{\rm ini}=0$  [Fig. 1(a)], the distribution

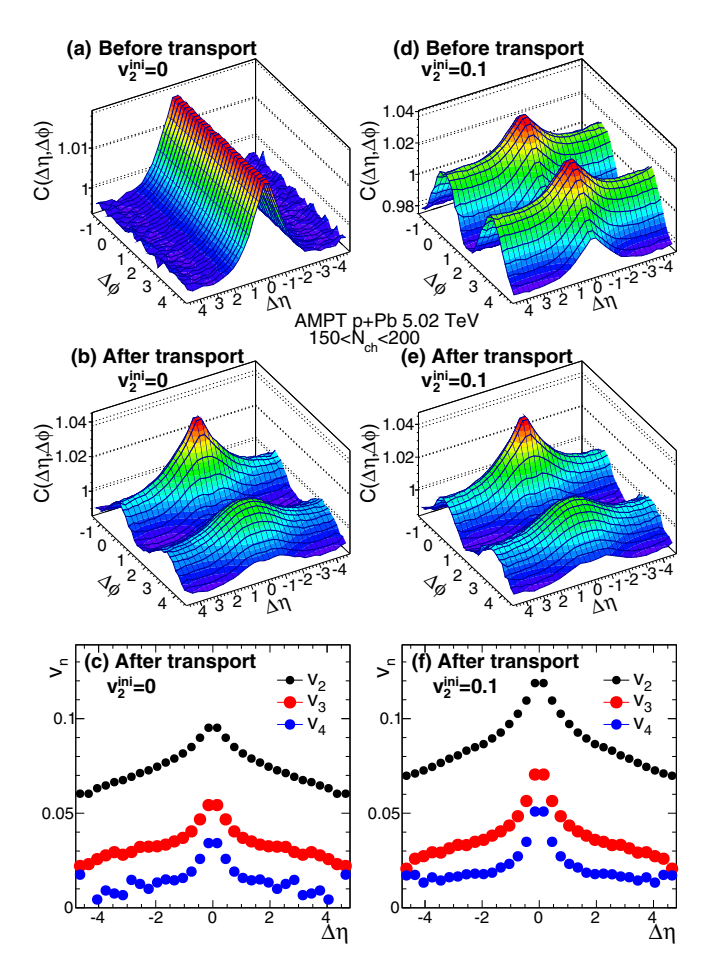


FIG. 1. The two-particle correlation in  $\Delta \phi$  and  $\Delta \eta$  for initial partons with  $v_2^{\rm ini}=0$  (top left) and  $v_2^{\rm ini}=0.1$  (top right) and for final partons after transport with  $v_2^{\rm ini}=0$  (middle left) and  $v_2^{\rm ini}=0.1$  (middle right). The bottom panels show the  $v_n(\Delta \eta)$  for n=2-4 calculated from the corresponding correlation functions in the middle panels.

is uniform in  $\Delta\phi$ . The peak around  $\Delta\eta=0$  reflects the short-range correlation which is randomized in  $\phi$  but is preserved in  $\eta$ . After the ZPC [Fig. 1(b)], an azimuthal anisotropy develops that appears as a double ridge at  $\Delta\phi\sim0$  and  $\Delta\phi\sim\pi$  extending to large  $\Delta\eta$ . On top of the double ridge are two short-range peaks with different amplitudes at the near and away sides. It is interesting to point out that without final-state interactions, such short-range azimuthal anisotropy, usually associated with "nonflow," would not show up in Fig. 1(b).

The azimuthal structure of the correlation function is quantified by the Fourier coefficients,  $v_n\{2\}^2 = \langle \cos n\Delta\phi \rangle$ , as a function of  $\Delta\eta$  in Fig. 1(c). The short-range structure in Fig. 1(b) is reflected by the narrow peak of  $v_n\{2\}$  around  $\Delta\eta=0$ , on top of a broad distribution associated with the double ridge in the correlation function. The short-range component in  $v_n\{2\}$  appears only after parton scatterings. The broad component in  $v_n\{2\}$  shows a slow decrease with  $\Delta\eta$ , which can be attributed to the longitudinal decorrelation effects [39,40].

In a transport picture, two partons with a large  $\eta$  separation are causally disconnected and should interact independently

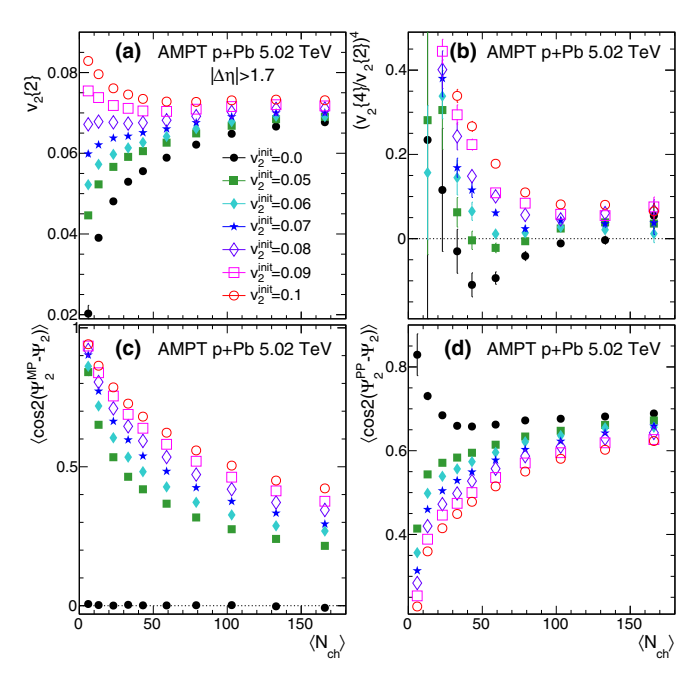


FIG. 2. The  $N_{\rm ch}$  dependence of final state flow  $v_2\{2\}$  (top left), the relative event-by-event flow fluctuation via cumulant ratio  $(v_2\{4\}/v_2\{2\})^4$  (top right), the angular correlation between the phase of final parton flow and the phase of initial momentum anisotropy (bottom left), and angular correlation between the phase of final parton flow and the PP (bottom right) for different input values of initial flow.

with the medium. Therefore, the azimuthal correlation between these two partons arises only through a response to a common geometry shape, leading to the long-range double ridge. For long-range correlations, this mechanism is indistinguishable from a geometry response driven by hydrodynamics. In contrast, the correlation of two partons close to each other in  $\eta$  is directly sensitive to the nonequilibrium microscopic scattering processes. The width of the short-range peak reflects the diffusion of the parton in rapidity via random scattering, in a way similar to hydrodynamic fluctuations [41]. The amplitude of the short-range peak reflects the amount of residual correlation not isotropized by the scattering process. Therefore, the long-range and the short-range correlations together can better constrain hydrodynamics or nonequilibrium transport: the long-range correlation constrains the overall strength of the geometry response, while the short-range correlation is sensitive to the nonequilibrium dynamics.

The right-hand column of Fig. 1 shows the case for  $v_2^{\rm ini} = 0.1$ . Despite the large initial momentum anisotropy, it only has a modest impact on the correlation function. The corresponding  $v_n$  values increase slightly at large  $|\Delta \eta|$ , while they increase more strongly at  $\Delta \eta \sim 0$ , such that the short-range peak is more evident.

To quantify the final azimuthal anisotropy after ZPC, we calculate the  $v_2\{2\}$  and  $v_2\{4\}$ , and study them as a function of  $N_{\rm ch}$ . To minimize multiplicity fluctuations, the results are calculated for events with the same  $N_{\rm ch}$  and then averaged to obtained results in a finite range of  $N_{\rm ch}$ . Figure 2(a) shows the  $N_{\rm ch}$  dependence of  $v_2\{2\}$ . When  $v_2^{\rm ini}=0$ , the  $v_2\{2\}$  values

show a monotonic increase with  $N_{\rm ch}$ , reflecting a dominant contribution from eccentricity-driven collective flow. However, as  $v_2^{\rm ini}$  is increased, the  $v_2\{2\}$  also increases. The increase is strongest at the low- $N_{\rm ch}$  region, and is weaker at the high- $N_{\rm ch}$  region. This behavior implies that at the low- $N_{\rm ch}$  region, initial momentum anisotropy dominates the collectivity after the ZPC. At the large- $N_{\rm ch}$  region, the initial momentum anisotropy still has up to a 10% contribution to the final  $v_2\{2\}$ .

Figure 2(c) shows the correlation between the phase for initial-state partons and the phase for final-state partons:  $\cos 2(\Psi_2^{\rm MP} - \Psi_2)$  [Eq. (9)]. At the low- $N_{\rm ch}$  region, the correlator is close to unity, suggesting that the initial momentum anisotropy can easily survive and dominate the final-state elliptic flow. At the high- $N_{\rm ch}$  region, the correlation decreases but is still quite large for the  $v_2^{\rm ini}$  values considered. This implies that the final parton's  $\Psi_2$  could be strongly biased by the initial momentum anisotropy.

Figure 2(d) shows the correlation between the phase of the initial eccentricity and phase of the elliptic flow of final-state partons:  $\langle\cos 2(\Psi_2^{\rm PP}-\Psi_2)\rangle$  [Eq. (8)]. When  $v_2^{\rm ini}=0$ , the correlation decreases with  $N_{\rm ch}$ , which can be attributed to the fact that  $\varepsilon_2$  values also decrease strongly with  $N_{\rm ch}$  [42]. It is more interesting to focus on the trend of the correlator when the  $v_2^{\rm ini}$  value is increased. For large  $v_2^{\rm ini}$ , the correlator value is dramatically decreased in the low- $N_{\rm ch}$  region, and the decrease is smaller at larger  $N_{\rm ch}$ . This suggests that the  $\Psi_2$  is more influenced by the initial momentum anisotropy in the low- $N_{\rm ch}$  region, but is less influenced in the high- $N_{\rm ch}$  region.

Finally, Fig. 2(b) shows  $(v_2\{4\}/v_2\{2\})^4$ , the cumulant ratio calculated via Eq. (7). The negative  $(v_2\{4\}/v_2\{2\})^4$  values simply imply that  $v_2\{4\}$  values become imaginary. The sign and  $N_{\rm ch}$ -dependent trend of this observable is found to depend on the  $v_2^{\rm ini}$ . In particular, large  $v_2^{\rm ini}$  could lead to a negative  $c_2\{4\}$  and therefore a real  $v_2\{4\}$  value. Results in Fig. 2(b) imply that the nature of the event-by-event flow fluctuation can be strongly modified in the presence of initial momentum anisotropy.

We have also checked dependence of the results in Fig. 2 on the choice of parameters in the AMPT model. It is found that reducing the partonic cross section leads to smaller  $v_2$  and stronger correlation with initial momentum anisotropy. The magnitude of  $(v_2\{4\}/v_2\{2\})^4$  also becomes larger. This is naturally expected since a smaller partonic cross section would produce less collectivity for final-state partons.

To further investigate the interplay between the initial momentum anisotropy and geometry-driven flow in the final state, two additional tests with  $v_2^{\rm ini}=0.05$  are carried out. In the first test, the phase of the initial flow  $\Psi_2^{\rm MP}$  is generated to align with the PP,  $\Psi_2^{\rm MP}=\Psi_2^{\rm PP}$ , while in the second test the  $\Psi_2^{\rm MP}$  is generated to be perpendicular to the PP:  $\Psi_2^{\rm MP}=\Psi_2^{\rm PP}+\pi/2$ . The results from these tests are shown in Fig. 3. When  $\Psi_2^{\rm MP}$  is aligned with the  $\Psi_2^{\rm PP}$ , final-state elliptic flow has larger values [Fig. 3(a)] and its correlations with both  $\Psi_2^{\rm MP}$  and  $\Psi_2^{\rm PP}$  are stronger [Figs. 3(c) and 3(d)], and the  $(v_2\{4\}/v_2\{2\})^4$  values are positive due to coherent enhancement of elliptic flow from  $v_2^{\rm ini}$  [Fig. 3(b)]. When  $\Psi_2^{\rm MP}$  is perpendicular to  $\Psi_2^{\rm PP}$ , opposite trends are observed: final-state elliptic flow has smaller values and its correlations with both

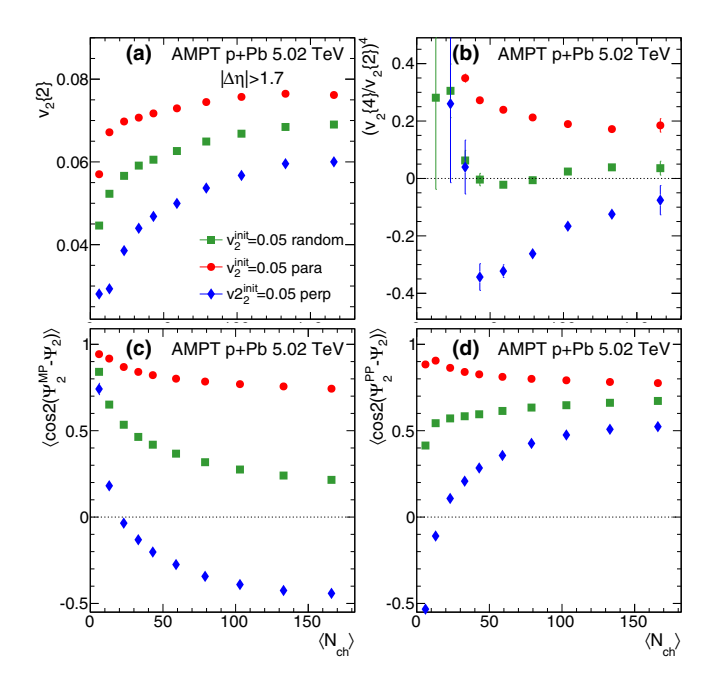


FIG. 3. The  $N_{\rm ch}$  dependence of final-state flow  $v_2\{2\}$  (top left), the relative event-by-event flow fluctuation via cumulant ratio  $(v_2\{4\}/v_2\{2\})^4$  (top right), the angular correlation between the phase of final parton flow and the phase of initial momentum anisotropy (bottom left), the angular correlation between the phase of final parton flow and the PP (bottom right) for input initial flow  $v_2^{\rm ini}=0.05$  with three different ways of generating the phase  $\Psi_2^{\rm MP}$ : random, parallel,  $\Psi_2^{\rm MP}=\Psi_2^{\rm PP}$ , and perpendicular,  $\Psi_2^{\rm MP}=\Psi_2^{\rm PP}+\pi/2$ .

 $\Psi_2^{\rm MP}$  and  $\Psi_2^{\rm PP}$  are weakened, and the  $(v_2\{4\}/v_2\{2\})^4$  values become negative.

Recently, the possibility for a further scan of small collision systems at RHIC and LHC was discussed [43–47]. The system scan at fixed  $\sqrt{s_{\rm NN}}$  varies mainly the size and shape of the initial fireball, while the RHIC-LHC energy scan for a fixed system such as O+O provides a setup with the same nucleon geometry but much larger parton densities at LHC. Therefore, such system and energy scans allow us to vary the role of initial momentum anisotropy, nonequilibrium transport, and hydrodynamics, and then to study the change in  $v_n$ . For example, the ordering of  $v_n$  at fixed  $N_{ch}$  between different systems or different energies can provide additional sensitivity on the initial momentum anisotropy, if such ordering does not follow the expected scaling from initial eccentricities [see Fig. 2(a)]. Furthermore, since the long-range correlation constrains the overall strength of the geometry response and the shortrange correlation constrains the nonequilibrium dynamics (see Fig. 1), a simultaneous study of the long-range and shortrange correlations can be used to disentangle two competing geometry response models based on nonequilibrium transport or hydrodynamics.

## IV. SUMMARY

In summary, we studied the influence of the initial momentum anisotropy on the geometry-driven collective flow in *p*+Pb collisions at 5.02 TeV using the AMPT model. We find that the initial momentum anisotropy may not be fully isotropized during partonic transport, and the final collective flow is correlated with directions of both the initial momentum anisotropy and the geometric eccentricity. The presence of initial momentum anisotropy also changes dramatically the strength of the event-by-event flow fluctuations. Therefore, the mere evidence of geometry response of the collective flow cannot rule out the presence of a large contribution from the initial state. A more comprehensive small system scan mapping out detailed pseudorapidity structures of two- and multiparticle correlation observables

is necessary to quantify the contributions from different scenarios.

### **ACKNOWLEDGMENTS**

We appreciate valuable discussion with Roy Lacey and Zhenyu Chen. This work is supported by NSF Grants No. PHY-1613294 and No. PHY-1913138, NSFC Grants No. 11828501, No. 11890714, No. 11835002, No. 11421505, 11890713 and No. 11961131011, the Key Research Program of the Chinese Academy of Sciences Grant No. XDPB09 and support of China Postdoctoral Science Foundation.

- [1] E. Shuryak, Rev. Mod. Phys. 89, 035001 (2017).
- [2] U. Heinz and R. Snellings, Annu. Rev. Nucl. Part. Sci. 63, 123 (2013).
- [3] S. A. Voloshin, A. M. Poskanzer, and R. Snellings, arXiv:0809.2949.
- [4] M. Luzum and H. Petersen, J. Phys. G 41, 063102 (2014).
- [5] J. Jia, J. Phys. G 41, 124003 (2014).
- [6] V. Khachatryan *et al.* (CMS Collaboration), J. High Energy Phys. 09 (2010) 091.
- [7] S. Chatrchyan *et al.* (CMS Collaboration), Phys. Lett. B 718, 795 (2013).
- [8] B. Abelev *et al.* (ALICE Collaboration), Phys. Lett. B **719**, 29 (2013).
- [9] G. Aad *et al.* (ATLAS Collaboration), Phys. Rev. Lett. 110, 182302 (2013).
- [10] G. Aad et al. (ATLAS Collaboration), Phys. Rev. C 90, 044906 (2014)
- [11] V. Khachatryan *et al.* (CMS Collaboration), Phys. Rev. Lett. 115, 012301 (2015).
- [12] M. Aaboud *et al.* (ATLAS Collaboration), Phys. Rev. C 97, 024904 (2018).
- [13] M. Aaboud *et al.* (ATLAS Collaboration), Phys. Lett. B 789, 444 (2019).
- [14] A. Adare *et al.* (PHENIX Collaboration), Phys. Rev. Lett. **111**, 212301 (2013).
- [15] A. Adare *et al.* (PHENIX Collaboration), Phys. Rev. Lett. **114**, 192301 (2015).
- [16] L. Adamczyk *et al.* (STAR Collaboration), Phys. Lett. B 747, 265 (2015).
- [17] C. Aidala *et al.* (PHENIX Collaboration), Phys. Rev. Lett. 120, 062302 (2018).
- [18] S. Huang (STAR Collaboration), Nucl. Phys. A 982, 475 (2019).
- [19] K. Dusling, W. Li, and B. Schenke, Int. J. Mod. Phys. E 25, 1630002 (2016).
- [20] F. Antinori et al., arXiv:1903.04289.
- [21] A. Kurkela, U. A. Wiedemann, and B. Wu, Eur. Phys. J. C 79, 965 (2019).
- [22] B. Schenke, Nucl. Phys. A 967, 105 (2017).
- [23] K. Dusling and R. Venugopalan, Phys. Rev. D **87**, 094034
- [24] M. Gyulassy, P. Levai, I. Vitev, and T. S. Biro, Phys. Rev. D 90, 054025 (2014).

- [25] B. Blok, C. D. Jäkel, M. Strikman, and U. A. Wiedemann, J. High Energy Phys. 12 (2017) 074.
- [26] M. Strickland, Acta Phys. Polon. B 45, 2355 (2014).
- [27] P. Romatschke and U. Romatschke, *Relativistic Fluid Dynamics In and Out of Equilibrium*, Cambridge Monographs on Mathematical Physics (Cambridge University Press, Cambridge, 2019).
- [28] L. Zhang, F. Liu, and F. Wang, Phys. Rev. C 92, 054906 (2015).
- [29] M. Greif, C. Greiner, B. Schenke, S. Schlichting, and Z. Xu, Phys. Rev. D 96, 091504(R) (2017).
- [30] Z.-W. Lin, C. M. Ko, B.-A. Li, B. Zhang, and S. Pal, Phys. Rev. C **72**, 064901 (2005).
- [31] A. Adare et al. (PHENIX Collaboration), Phys. Rev. C 94, 054910 (2016).
- [32] G.-L. Ma and A. Bzdak, Phys. Lett. B 739, 209 (2014).
- [33] A. Bzdak and G.-L. Ma, Phys. Rev. Lett. **113**, 252301 (2014).
- [34] M.-W. Nie, P. Huo, J. Jia, and G.-L. Ma, Phys. Rev. C 98, 034903 (2018).
- [35] M. Masera, G. Ortona, M. G. Poghosyan, and F. Prino, Phys. Rev. C 79, 064909 (2009).
- [36] J. Jia, M. Zhou, and A. Trzupek, Phys. Rev. C 96, 034906 (2017).
- [37] G. Giacalone, J. Noronha-Hostler, and J.-Y. Ollitrault, Phys. Rev. C 95, 054910 (2017).
- [38] M. Zhou and J. Jia, Phys. Rev. C 98, 044903 (2018).
- [39] P. Bozek, W. Broniowski, and J. Moreira, Phys. Rev. C 83, 034911 (2011).
- [40] M. Aaboud *et al.* (ATLAS Collaboration), Eur. Phys. J. C **78**, 142 (2018).
- [41] A. Sakai, K. Murase, and T. Hirano, JPS Conf. Proc. 26, 031022 (2019).
- [42] P. Bozek, Phys. Rev. C 85, 014911 (2012).
- [43] M. Rybczyński, M. Piotrowska, and W. Broniowski, Phys. Rev. C 97, 034912 (2018).
- [44] Z. Citron et al., arXiv:1812.06772.
- [45] M. D. Sievert and J. Noronha-Hostler, Phys. Rev. C 100, 024904 (2019).
- [46] S. H. Lim, J. Carlson, C. Loizides, D. Lonardoni, J. E. Lynn, J. L. Nagle, J. D. Orjuela Koop, and J. Ouellette, Phys. Rev. C 99, 044904 (2019).
- [47] S. Huang, Z. Chen, J. Jia, and W. Li, arXiv:1904.10415.